Sensors & Transducers, Vol. 245, Issue 6, October 2020, pp. 99-104

www.sensorsportal.com

Sensors & Transducers

Published by IFSA Publishing, S. L., 2020
http://www.sensorsportal.com

Analysis of Backscattering Data from Closely Spaced Scatterers Using the K Matrix Information

[1] Maria STAN NECULA, [1, 2, *] Dorin BIBICU and [1] Luminita MORARU

[1] University 'Dunărea de Jos' of Galați, Romania, Modelling & Simulation Laboratory, 111 Domneasca St., 800201 Galati, Romania

[2] University 'Dunărea de Jos' of Galați, Romania, Business Administration Department, 59-61 N. Balcescu St., 800001 Galati, Romania

[1] Tel.: + 40 336 130 251, fax: + 40 236 319 329

[*] E-mail: dorin.bibicu@ugal.ro

Received: 7 September 2020 /Accepted: 15 October 2020 /Published: 30 October 2020

Abstract: A coincident array of N transceivers is used to estimate the location of a multitude of closely spaced scatterers under arbitrary wave propagation conditions. MUltiple SIgnal Classification (MUSIC) algorithm analyses a multitude of scatterers placed in specific geometries. The formulation of the inverse scattering problem and the multistatic data matrix K are defined in two approximations: the Foldy-Lax (FL) formulation of the full multiple scattering model and the distorted-wave Born approximation (DWBA) model. The Fréchet distances (FD) between the amplitude and phase curves derived from K matrix data and of the amplitude of the scattered signals estimates the effectiveness of the approximation methods. The numerical results showed a slight effectiveness of the Foldy-Lax approximation for scatterers location. The problem of considering the phase estimation from the K matrix is not a solution for signal reconstruction and representation.

Keywords: Inverse scattering, Foldy-Lax formulation, Distorted-wave Born approximation, MUSIC, Fréchet distance, Average visibility index.

1. Introduction

The MUltiple SIgnal Classification (MUSIC) is a method applied to locate a number of small targets with arbitrary locations. MUSIC operates based on the assumption that the far field patterns of point sources are almost orthogonal to the noise subspace of the far field operator or so called multistatic matrix data K. K is obtained for a collection of M targets and an active array of N transceivers [1-6]. Gruber, *et al.* [1] established that the MUSIC is able to locate point targets using both the Born approximation and more general scattering models that consider multiple scattering processes between the targets. The MUSIC algorithm takes in as input a K matrix which is approximated using two approximations: the Foldy-Lax (FL) formulation of the multiple scattering model [7-10] and the distorted-wave Born approximation model (DWBA) [11, 12]. The FL considers the multiple scattering among the scatterers but the self-interactions at the target locations are excluded. DWBA ignores this multiple scattering among the scatterers effect.

Therefore, the aims of this paper are to evaluate the accuracy of target location using the values of phase and amplitude provided by the K matrix, and the amplitude of scattered signals provided by the MUSIC pseudospectrum in the far-field condition. The issue of interest is to have either closely spaced targets and/or sparse transceiver arrays. The targets are placed in a

background medium with known properties. The formulation of the inverse scattering problem is defined under the FL and DWBA approximation methods. More specific, we formulate the K matrix in these two approximations and the MUSIC algorithm takes in as input these K matrices. Neither approximation intends to recover the type or properties of these scatterers. In our case, we are focusing on the data collected at 5, 10, 50 and 100 Hz (or normalized wavelengths of 1, 0.5, 0.1, and 0.05) in order to develop a new scanning technology applicable in a nondivest and noncontact condition. Additive white Gaussian noise (AWGN) is used to investigate the noise immunity and the noise-free case is presented for comparison purpose. A new aspect is addressed here: the investigation of the amplitude and phase distribution of the singular vectors obtained from the SVD of the matrix K in both approximations through the Fréchet distance measurement in order to quantify the distance between the amplitude and phase curves vs. the number of transceivers in both approximations [13-15]. The proper scatterer detection is provided by these target geometries and set of parameters, which minimize the Fréchet distance and maximize the amplitude of the reconstructed signal.

This problem has a practical implementation in sonar systems, medicine and ultrasound imaging, nondestructive testing, and smart fighting methods against border smuggling through hidden object detection, as this paper intended to investigate.

The rest of this paper is organized as follows: Section 2 is devoted to the problem statement (a theoretical framework for MUSIC and approximation models and the selection algorithm). Section 3 presents the results, which are discussed in Section 4. Finally, conclusions are presented in Section 5.

2. Materials and Methods

2.1. Inverse Scattering Problem Formulation

2.1.1. Foldy-Lax Formulation

The sum of the scattered field and the incident field for the kth transceiver build the total field:

$$u_k(\mathbf{r})=u_k^{inc}(\mathbf{r})+\sum_{m=1}^{M}\tau_m G_0(\mathbf{r}, \mathbf{x}_m)\, u_k(\mathbf{x}_m), \quad (1)$$

where $\tau_m > 0$ denotes the target scattering strength for a m^{th} point scatterer, and G_0 is the background Green function that is defined as, for a scatterer locations $r = x_m$:

$$G_0(r, r')=\frac{e^{ik|r-r'|}}{4\pi|r-r'|} \quad (2)$$

In the case of a collection of M point scatterers located at x_m, m = 1, 2, …, M, the FL model for the scattered wave field when the self-interactions at the target locations are excluded, is [7, 16, 17].

$$u_k(x_m)=u_k^{inc}(x_m)+\sum_{m\neq m'}\tau_{m'}G_0(x_m, x_{m'})u_k(x_{m'}) \quad (3)$$

The FL model hypothesis that the data on the incident field u_k^{inc}, scatterer locations x_m, and target scattering strength τ_m are known. A coincident array meets the condition j = k = N, and (1) and (3) became

$$G(x_m, \alpha_k) = G_0(x_m, \alpha_k) + \sum_{m'\neq m}\tau_{m'}G_0(x_m, x_{m'})G(x_{m'}, \alpha_k), \quad (4)$$

where $G(r, \alpha_k)$ is a complete Green function of the combined background with the addition of the target medium for a source point $r' = \alpha_k$ at the kth emitter and, similarly, $G(\alpha_j, r)$ for the j^{th} receiver location. The K matrix in the FL approximation is:

$$K^{FL} = \sum_{m=1}^{M}\tau_m G_0(\alpha_j, x_m)G(x_m, \alpha_k) = \sum_{m=1}^{M}\tau_m G_0(x_m, \alpha_j)G(x_m, \alpha_k), \quad j = 1, \ldots, M; k = 1, \ldots, N \quad (5)$$

The matrix Formulation (5) is a correction of Green's function accounting for the scattering of considered targets.

2.1.2. Distorted-wave Born Approximation (DWBA) Model

The DWBA model is a tool for weak scatterers analysis [11]. When the scattering targets have acoustic properties different from the background medium, then the DWBA model is as follows:

$$G(\mathbf{x_m}, \alpha_j)\approx G_0(\mathbf{x_m}, \alpha_j) \quad (6)$$

The multistatic scattering matrix within the DWBA approximation is

$$K^{DWBA}=\sum_{m=1}^{M}\tau_m G_0(\mathbf{x_m}, \alpha_j)G_0{}^{T}(\mathbf{x_m}, \alpha_k) \quad (7)$$

DWBA estimates the target locations from the multistatic scattering matrix when the condition M < N is met. In addition, this is a requirement related to well-separated scatterers so they are 'viewed' by the transceiver array. However, DWBA is only relevant at small incident angles and at small exit/reflection angles.

2.2. MUSIC Algorithm

The MUSIC algorithm uses the SVD of K matrix and both discrete version of the multistatic scattering matrix (5) and (7) to define the wave scattering amplitude [18]. For M point scatterers located at $\mathbf{x}_m=\{x_1, \ldots x_M\}\in R^3$ and when N ≥ M, two matrices S_{jm}, j = 1, …, N, j = 1, …, N and m = 1, …, M consisting of the background Green function vectors computed at the scatterer locations and $\mathbf{T}=\text{diag}(\tau_m)$ are defined so that the multistatic matrix is $K=S\mathbf{T}S^*$. denotes the adjoint of S. MUSIC characterizes the range of a self-adjoint operator. When nonstationary signals are analyzed, a better approach is singular value decomposition. SVD reduces a matrix to its constituent parts and ensures an orthogonal basis for the signal space of the matrix. The eigenvectors of K provide information on the scatterers, and SVD determines the number of inclusions in the propagation space. K can be transformed into a Hermitian matrix using the frequency-domain version of a time-reversed multistatic response matrix. Further, the eigenvectors and corresponding eigenvalues of the Hermitian multistatic scattering matrix are computed using SVD. SVD is more stable than the standard eigenvalue method [19]. These statements are essential observations of the MUSIC approach. This means that one can estimate the locations of the scatterers associated with the received signals by finding those steering vectors f(x), which are most nearly orthogonal in the null (noise) space.

2.3. Fréchet Distance

The Fréchet distance (FD) is a measure of the similarity between two parametrized curves X and Y defined in R^n [13, 14]:

$$\text{FD}(X,Y) = \min_{\substack{a:[0,1]\to[0,N] \\ b:[0,1]\to[0,M]}} \left\{ \max_{t\in[0,1]} d\big(X(a(t)), Y(b(t))\big) \right\}, \quad (8)$$

where a(t) and b(t) are parametrized functions with a(0) = 0, a(1) = N, b(0) = 0, and b(1) = M. d(·,·) is a common distance metric such as the Hausdorff or Euclidian distance. We must mention that these common distance metrics are not suitable for estimating the similarity between two curves because they simply measure the distance between points in a set of points but fail to consider the structure of the curves and the point correlations in the same set. FD indicates matches between the analyzed curves by computing the distance between a point traveling along the X curve and a point traveling along the Y curve. Usually, each point can travel at a different speed on each curve.

The FD between the amplitude and phase curves plotted using the data provided by the singular vectors obtained from the SVD of the matrix K in the FL and DWBA approximations is determined. The best target locations are provided by the smaller values of FD.

2.4. Proposed Algorithm

The target location problem is investigated for four spatial distribution geometries. The MUSIC algorithm for both approximations provides reconstruction methods that depend on the choice of the signal and noise subspaces of the multistatic scattering matrix. For small measurement noise n1 or for higher SNR it is easy to choose these subspaces and to detect and locate the scatterers in a finer way. A small amount of noise depicts almost ideal conditions whereas a large amount of noise n2 will strongly disturb the detection of the scatterers. The algorithm is as follows:

Step 1: Define the set of parameters as p:{λ, n1, n2}, where n1 and n2 denote AWGNs having a variance of 0.0009 and 0.09, respectively;

Define the results as r:$\{ FD^{FL}_{amplitude}, FD^{DWBA}_{amplitude}, FD^{FL}_{phase}, FD^{DWBA}_{phase}\}$, where λ = (1, 0.5, 0.1, 0.01) and P = (noise-free, n1, n2) (see Table 1);

Step 2: Generate all possible combinations, the experimental parameters and results are distributed into six lists: $L1 = \{\lambda, P, FD^{FL}_{amplitude}\}$, $L2 = \{\lambda, P, FD^{DWBA}_{amplitude}\}$, $L3 = \{\lambda, P, FD^{FL}_{phase}\}$, $L4 = \{\lambda, P, FD^{DWBA}_{phase}\}$;

Step 3: Extract the smallest FD values from the first four lists Li (I = 1:4) and generate the FD list $FD^{FL}_{amplitude}$, FD^{FL}_{phase}, $FD^{DWBA}_{amplitude}$, FD^{DWBA}_{phase}} (see data in Tables 2 and 3);

Step 4: Run steps 2 and 3 for 16 times for each target distribution; 64 measurements are made.

3. Results

3.1. Simulation Framework

The simulation approach was implemented in the MATLAB 2017b environment [20]. The following parameters were used:

- N = 10 transceivers in a coincident linear array located at (-20,0), (-15,0), (-10,0), (-5,0), and (-2,0). The targets are located as follows: triangle (T): (0,-8), (-1,-9), (1,-9), (-2,-10), (0,-10) and (2,-10); parallelogram (P): (-2,-8), (0,-8), (2,-8), (0,-9), (2,-9) and (4,-9); diamond (D): (0,-6), (-2,-8), (0,-10), (2,-8), (0,-7) and (0,-9); and ellipse (E): (0,-8), (-3,-9), (3,-9), (-3,-10), (3,-10) and (0,-11);
- M = 6 closely spaced scatterers having a spatial distribution into triangle (T), parallelogram (P), diamond (D), and ellipse (E) geometries. The target scattering strength is τ = (1, 1.3, 1.6, 1.6, 1.3, 1);
- AWGN with variances of 0.0009 and 0.09 is added; noise disturbs the multistatic scattering matrices K^{FL} and K^{DWBA} and results in various signal-to-noise (SNR) values. In addition, the noise-free case is considered.

These parameters maintain the computational time within reasonable limits.

A block diagram of the proposed method is displayed in Fig. 1.

3.2. Results

Fig. 2 displays plots transceiver and target locations. Both the phase and amplitude distribution of the singular vectors obtained from SVD of matrix K in FL and DWBA methods are presented in Fig. 3.

FD estimates the errors of the approximate solutions of the data provided by the singular vectors obtained from SVD of the matrix K, and allows the establishment of an efficient geometry of the target localization. According to the data presented in Table 1, the smallest $FD_{amplitude}$ values indicate an improvement in the FL approximation.

Table 1. Average $FD_{amplitude}$ and FD_{phase} values and amplitude (A) of scattered signals attained in simulation experiments for 2D obstacles, extracted from list Li (i = 1:6), for FL and DWBA approximations.

Geometry	AWGN noise	SNR (dB)	$FD^{FL}_{amplitude}$	$FD^{DWBA}_{amplitude}$	FD^{FL}_{phase}	FD^{DWBA}_{phase}
(T)	n1	22.38	$0.18 \cdot 10^{-3}$	0.0002	3.035	3.1249
	n2	6.3	0.2168	0.2183	2.946	3.0001
(P)	n1	22.66	$0.21 \cdot 10^{-3}$	0.0103	0.278	0.2875
	n2	8.9	0.2222	0.2225	2.216	2.2747
(D)	n1	22.12	$0.18 \cdot 10^{-3}$	0.0003	0.157	0.2192
	n2	3.3	0.2210	0.2212	3.701	3.7075
(E)	n1	21.62	$0.13 \cdot 10^{-3}$	0.0001	1.896	0.2143
	n2	9.32	0.22068	0.2205	2.001	2.0671

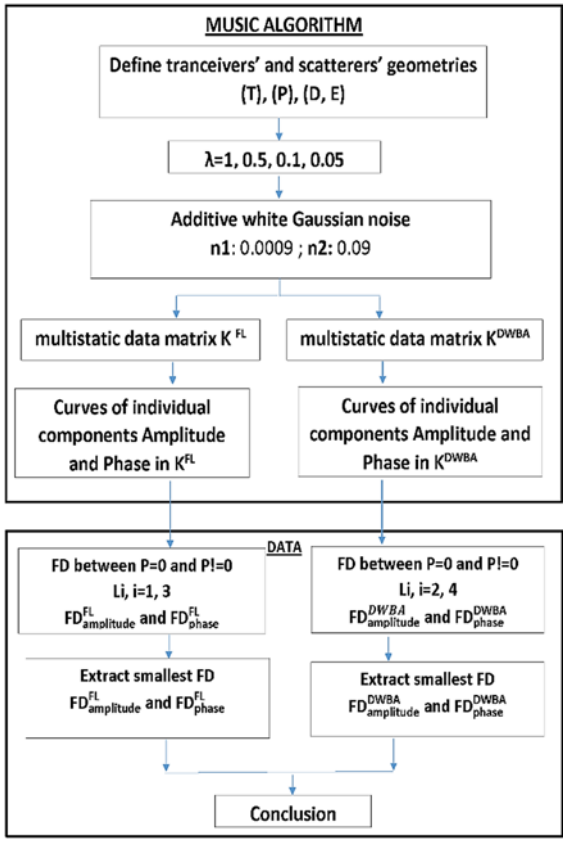

Fig. 1. Block diagram.

As expected, the case of noise-free scattering returns the same results. By contrast, the noisy experiment indicates that DWBA provided somewhat worse results in terms of the FDs and amplitude values of the reconstructed signals. The exception is the ellipse spatial distribution for noise n2, where almost similar results were obtained.

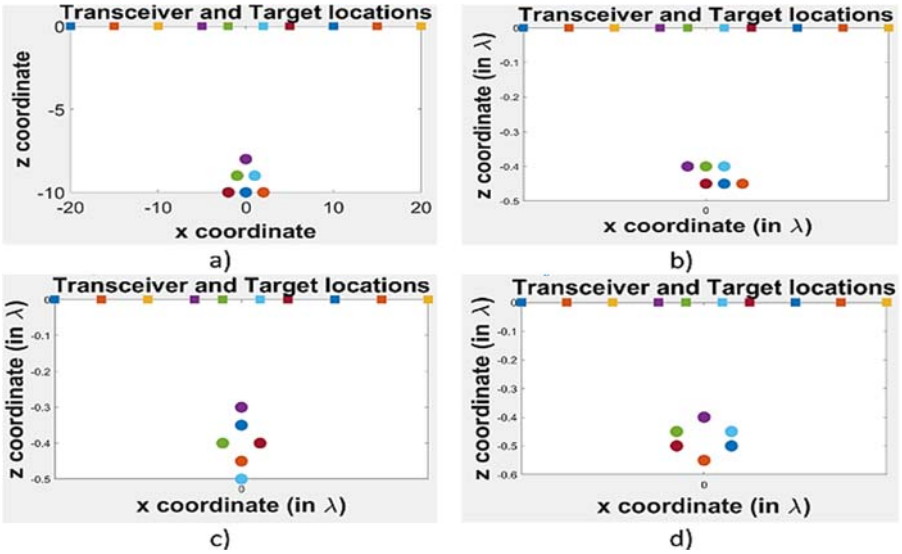

Fig. 2. Problem setup: 10 transceivers (depicted as squares) and 6 targets (depicted as circles) are embedded in uniform background. Targets' spatial distributions are represented as a) Triangle (T); b) Parallelogram (P); c) Diamond (D), and d) Ellipse (E).

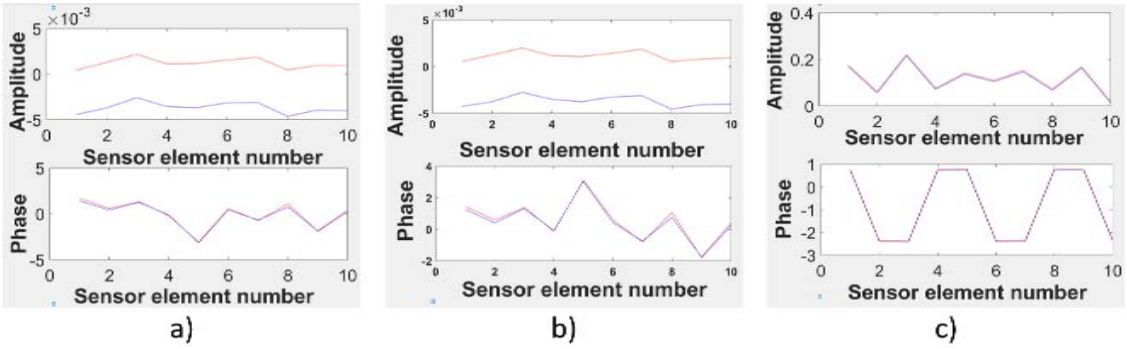

Fig. 3. Curves of individual components: 'amplitude' (top) and 'phase' (bottom) provided by the left singular vectors obtained from SVD of the matrix K in FL approximation (blue) and DWBA approximation (red) vs. number N = 10 of array elements in triangle (T) geometry and for λ = 1. a) Noise-free, b) n1, c) n2.

The $FD_{amplitude}$ for both approximations (Table 1) shows a variability with the wavelength and spatial distribution of the targets. Diamond (D) and ellipse (E) distributions have smaller $FD_{amplitude}$ values when a comparison between approximations is performed (Table 2). The FL approximation shows a fair robustness against noise, while DWBA drives an unstable reconstruction process. On the other hand, FD_{phase} remains almost unchanged with no contribution to the optimization problem regardless of the targets' spatial distributions (Tables 1 and 2).

Table 2. Ratio of AWGN noise-added (n1 and n2) to noise-free values for smallest $FD^{FL}_{amplitude}$ and $FD^{DWBA}_{amplitude}$ values across various spatial distributions and wavelengths.

Noise-free vs. n1					
λ	**Geometry**	$\mathbf{FD^{FL}_{amplitude}}$	**λ**	**Geometry**	$\mathbf{FD^{DWBA}_{amplitude}}$
0.5	(P)	$0.20 \cdot 10^{-3}$	1	(D)	$0.94 \cdot 10^{-3}$
0.5	(T)	$0.23 \cdot 10^{-3}$	0.5	(E)	$0.33 \cdot 10^{-3}$
Noise-free vs. n2					
1	(E)	0.020	1	(E)	0.022
1	(D)	0.042	1	(D)	0.062

4. Discussion

The formulation of the inverse scattering problem is defined under FL and DWBA approximation methods. The K matrix is generated via these approximations. SVD identifies the right singular and the left singular vectors associated to the singular value decomposition of K. The plots the amplitude and phase distribution of the singular vectors are analyzed using the Fréchet distance. Simulated data shows that the Fréchet distance values are affected by the target locations and their spatial distributions, normalized wavelengths, and noise (Fig. 3 and Table 1). Noise disturbs the multistatic scattering matrices K^{FL} and K^{DWBA} and acoustic field distribution.

Data displayed in Fig. 3 and Tables 1-3 indicates that the 'phase' provided by the singular vectors obtained from SVD of the matrix K is not dramatically affected by the location of the targets. The 'amplitude' in matrix K is more affected by changes in the target location. In addition, the distribution of the 'amplitude' FD and 'phase' FD components in K (Table 1) shows variability for each wavelength, although there is no FD-wavelength relationship. Smaller FD values indicate a higher similarity between curves and allows for estimating the validity of the approximation model. Moreover, for each target's geometry, the SNR values are almost similar for the same experimental conditions. This indicates that it is quite difficult and expensive to obtain the 'phase' and 'amplitude' data in the SDV singular vectors of the K matrix, under these experimental conditions.

Table 3. Ratio of AWGN noise-added (n1 and n2) to noise-free values for FD^{FL}_{phase} and FD^{DWBA}_{phase} smallest values across various spatial distributions and wavelengths.

Noise-free vs. n1					
λ	**Geometry**	$\mathbf{FD^{FL}_{phase}}$	**λ**	**Geometry**	$\mathbf{FD^{DWBA}_{phase}}$
0.5	(T)	0.010	1	(D)	0.011
0.5	(D)	0.021	0.5	(E)	0.024
Noise-free vs. n2					
1	(D)	1.143	1	(E)	2.958
1	(P)	2.015	1	(D)	2.106

5. Conclusions

This work investigated questions related to a new scanning technology applicable in a nondivest and noncontact condition based on the inverse scattering of point scatterers embedded in a known background environment. We are currently working on a low-frequency interrogation technology for a possible contactless patdown system based on the automatic detection of external concealed commodities viewed as scatterers or targets.

The inverse scattering problem was approached using two well-known approximations: FL formulation of the multiple scattering model and the DWBA model. The K matrix was generated using these approximations and has two different mathematical forms depending on the used approximation. The singular vectors obtained from the SVD of the matrix K in FL and DWBA approximations and the Fréchet distance were used to estimate the similarity between the 'amplitude' and 'phase' curves of the K matrix. The best target location was determined by minimizing the values of FD.

The numerical results showed a slight effectiveness of the Foldy-Lax approximation for scatterers location. The problem of considering the phase estimation from the K matrix is not a solution for signal reconstruction and representation. However, our results indicated that the efficiency of the target location marginally depends on the placement of the interior points and strongly depends on the wavelength and level of noise.

Acknowledgements

The work of the first author was partially supported by the European Social Fund - the Sectoral Operational Programme Human Capital 2014-2020, through the Financial Agreement with the title "Burse pentru educaţia antreprenorială în rândul doctoranzilor şi cercetătorilor postdoctorat (Be Antreprenor!)" (in Romanian) or "Scholarships for entrepreneurial education among doctoral students and postdoctoral researchers (Be Entrepreneur!)", Contract no. 51680/09.07.2019 - SMIS code: 124539.

References

[1]. F. K. Gruber, E. A. Marengo, A. J. Devaney, Time-reversal imaging with multiple signal classification considering multiple scattering between the targets, *Journal of the Acoustical Society of America*, Vol. 115, Issue 6, 2004, pp. 3042-3047.

[2]. E. A. Marengo, F. K. Gruber, Noniterative analytical formula for inverse scattering of multiply scattering point targets, *Journal of the Acoustical Society of America*, Vol. 120, Issue 6, 2006, pp. 3782-3788.

[3]. C. Prada, J. L. Thomas, Experimental subwavelength localization of scatterers by decomposition of the time-reversal operator interpreted as a covariance matrix, *Journal of the Acoustical Society of America*, Vol. 114, Issue 1, 2003, pp. 235-243.

[4]. D. Bibicu, M. Necula (Stan), L. Moraru, Acoustic radiation from baffled vibrating plates with various geometries, *AIP Conference Proceedings*, Vol. 2071, Issue 1, 2019, 040009.

[5]. M. Necula (Stan), D. Bibicu, L. Moraru, Backscattering problems by a non-convex kite-shape objects in acoustic frequency domain, *AIP Conference Proceedings*, Vol. 2071, Issue 1, 2019, 040008.

[6]. D. Ciuonzo, P. S. Rossi, Noncolocated time-reversal MUSIC: High-SNR distribution of null spectrum, *IEEE Signal Processing Letters*, Vol. 24, Issue 4, 2017, pp. 397-401.

[7]. L. L. Foldy, The multiple scattering of waves. I. General theory of isotropic scattering by randomly distributed scatterers, *Physical Review*, Vol. 67, 1945, pp. 107-119.

[8]. M. Lax, Multiple scattering of waves, *Review Modern Physical*, Vol. 23, 1951, pp. 287-310.

[9]. M. Lax, Multiple scattering of waves II. The effective field in dense systems, *Physical Review*, Vol. 85, 1952, pp. 261-269.

[10]. K. Huang, K. Solna, H. Zhao, Generalized Foldy–Lax formulation, *Journal Computational Physics*, Vol. 229, Issue 12, 2010, pp. 4544-4553.

[11]. D. Chu, K. G. Foote, T. K. Stanton, Further analysis of target strength measurements of Antarctic krill at 38 and 120 kHz: Comparison with deformed cylinder model and inference of orientation distribution, *The Journal of the Acoustical Society of America*, Vol. 93, Issue 5, 1993, pp. 2985-2988.

[12]. B. A. Jones, A. C. Lavery, T. K. Stanton, Use of the distorted wave born approximation to predict scattering by inhomogeneous objects: application to squid, *The Journal of the Acoustical Society of America*, Vol. 125, Issue 1, 2009, pp. 73-88.

[13]. K. Buchin, M. Buchin, Y. Wang, Exact algorithms for partial curve matching via the Fréchet distance, in *Proceedings of the 20th Annual ACM-SIAM Symposium on Discrete Algorithms,* 2009, pp. 645-654.

[14]. A. Driemel, S. Har-Peled, C. Wenk, Approximating the Fréchet distance for realistic curves in near-linear time, *Discrete and Computational Geometry*, Vol. 48, Issue 1, 2012, pp. 94-127.

[15]. M. de Berg, A. F. Cook, J. Gudmundsson, Fast Fréchet queries, *Computational Geometry: Theory and Applications*, Vol. 46, Issue 6, 2013, pp. 747-755.

[16]. K. Huang, P. Li, A two-scale multiple scattering problem, *Multiscale Modeling Simulation*, Vol. 8, Issue 4, 2010, pp. 1511-11534.

[17]. K. Huang, K. Solna, H. Zhao, Generalized Foldy–Lax formulation, *Journal of Computational Physics*, Vol. 229, Issue 12, 2010, pp. 4544-4553.

[18]. A. Kirsch, The MUSIC-algorithm and the factorization method in inverse scattering theory for inhomogeneous media, Inverse Problems, Vol. 18, Issue 4, 2002, pp. 1025-1040.

[19]. S. Gu, J. Ni, J. Yuan, Non-stationary Signal Analysis and Transient Machining Process Condition Monitoring, International Journal Mach Tools and Manufactures, Vol. 42, Issue 1, 2002, pp. 41-51.

[20]. MathWorks. Available online: (https://www.mathworks.com/help/signal/ref/spectrum.music.html (accessed on 11 March 2020).